Supplementary Information for:

Determination of Isosteric Heat of Adsorption by Quenched Solid Density Functional Theory

Richard T. Cimino[1], Piotr Kowalczyk[2], Peter I. Ravikovitch[3], and Alexander V. Neimark[1†]

[1]*Dept. of Chemical and Biochemical Engineering, Rutgers University, Piscataway, NJ 08854, USA*
[2]*School of Engineering and Information Technology, Murdoch University, Perth, WA, 6150 Australia*
[3]*ExxonMobil Research and Engineering Company, Annandale, NJ 08801, USA*

A. QSDFT Kernels for Ar adsorption on silica

A total of four QSDFT kernels were created for this work for Ar adsorption in cylindrical silica pores. These kernels consist of equilibrium and adsorption isotherms at 77.4 and 87.3K. The cylindrical-shaped pores range in diameter from 1 to $30\sigma_{ff}$ (0.34-10nm). This pore range is sufficient to capture the adsorption behavior in mesoporous MCM-41, which typically consists of mesopores ≤ 5nm. Example kernel isotherms for kernel K1 are shown below in **Fig. S1.**

(K1) Equilibrium adsorption kernel Ar @ 87.3K – cylindrical pore model, silica QSDFT

Kernel consisting of 194 cylindrical geometry, equilibrium isotherms in the pore size range 0.35 – 10 nm with a grid spacing 0.05 nm apart. Temperature 87.29K. Relative pressure range 10^{-9} to 1.09 with a grid of 135 pressure points on a logarithmic scale.

(K2) Adsorption kernel Ar @ 87.3K – cylindrical pore model, silica QSDFT

Kernel consisting of 93 cylindrical geometry, equilibrium isotherms in the pore size range 0.35 – 4.5 nm with a grid spacing 0.05 nm apart and 101 cylindrical geometry, adsorption isotherms in the pore size range 5.0 – 10 nm with a grid spacing 0.05 nm apart. Temperature 87.29K. Relative pressure range 10^{-9} to 1.09 with a grid of 135 pressure points on a logarithmic scale.

(K3) Equilibrium adsorption kernel Ar @ 77.4K – cylindrical pore model, silica QSDFT

Kernel consisting of 194 cylindrical geometry, equilibrium isotherms in the pore size range 0.35 – 10 nm with a grid spacing 0.05 nm apart. Temperature 77.355K. Relative pressure range 10^{-9} to 1.09 with a grid of 135 pressure points on a logarithmic scale.

(K4) Adsorption kernel Ar @ 77.4K – cylindrical pore model, silica QSDFT

Kernel consisting of 93 cylindrical geometry, equilibrium isotherms in the pore size range 0.35 – 4.5 nm with a grid spacing 0.05 nm apart and 101 cylindrical geometry, adsorption isotherms in the pore size range 5.0 – 10 nm with a grid spacing 0.05 nm apart. Temperature 77.355K. Relative pressure range 10^{-9} to 1.09 with a grid of 135 pressure points on a logarithmic scale.

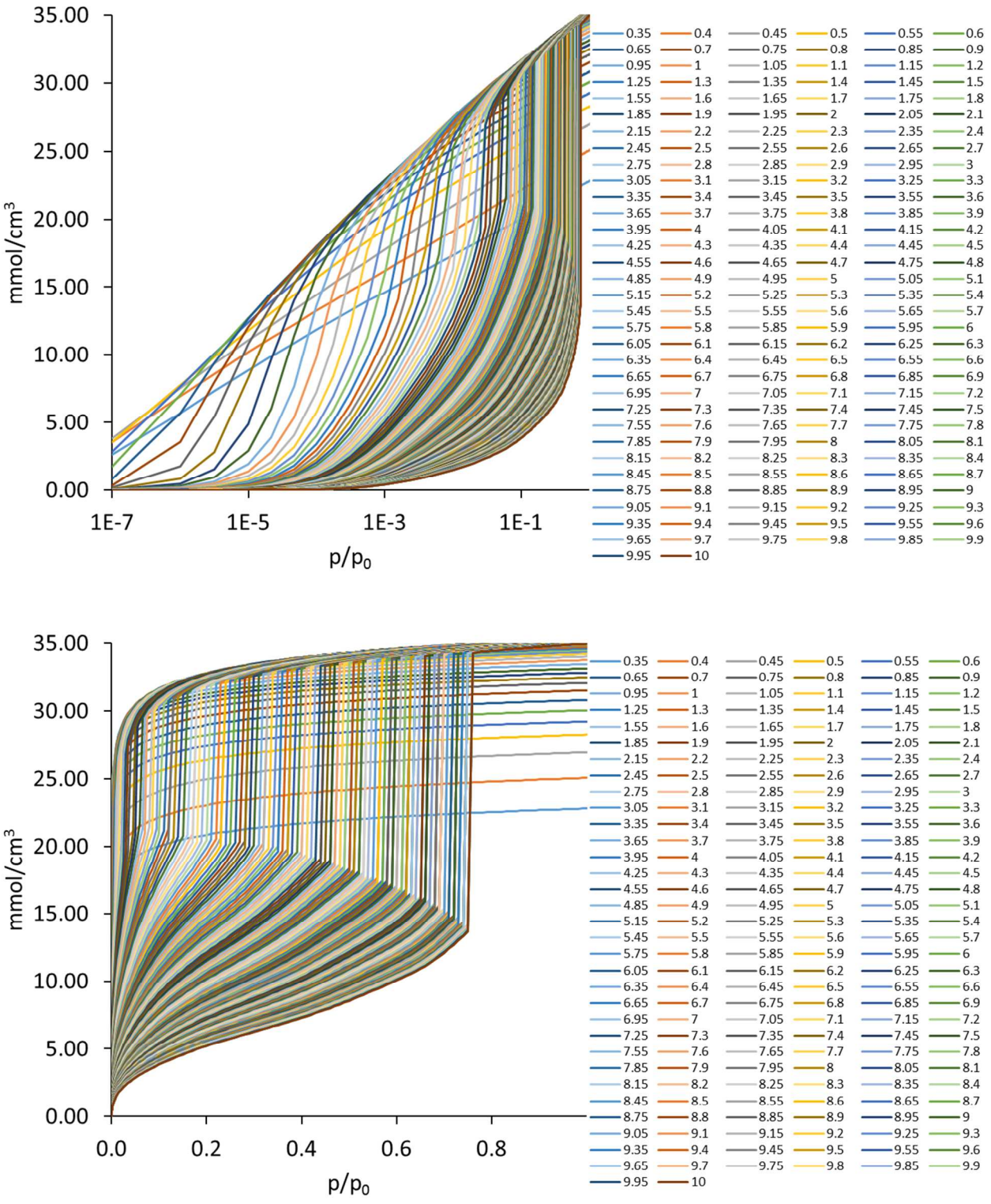

Fig. S1. Isotherm kernel for K1 in logarithmic and normal pressure coordinates.

B. Details of isosteric heat calculation algorithm using one isotherm

A schematic of the process for determining the isosteric heat of adsorption for a porous material is presented below in **Fig. S2**, to accompany the primary description in the main text. The example given in the figure corresponds to AM-5 carbon (Fig. 6 in the main text), T_1 = 87K and T_2 = 77K.

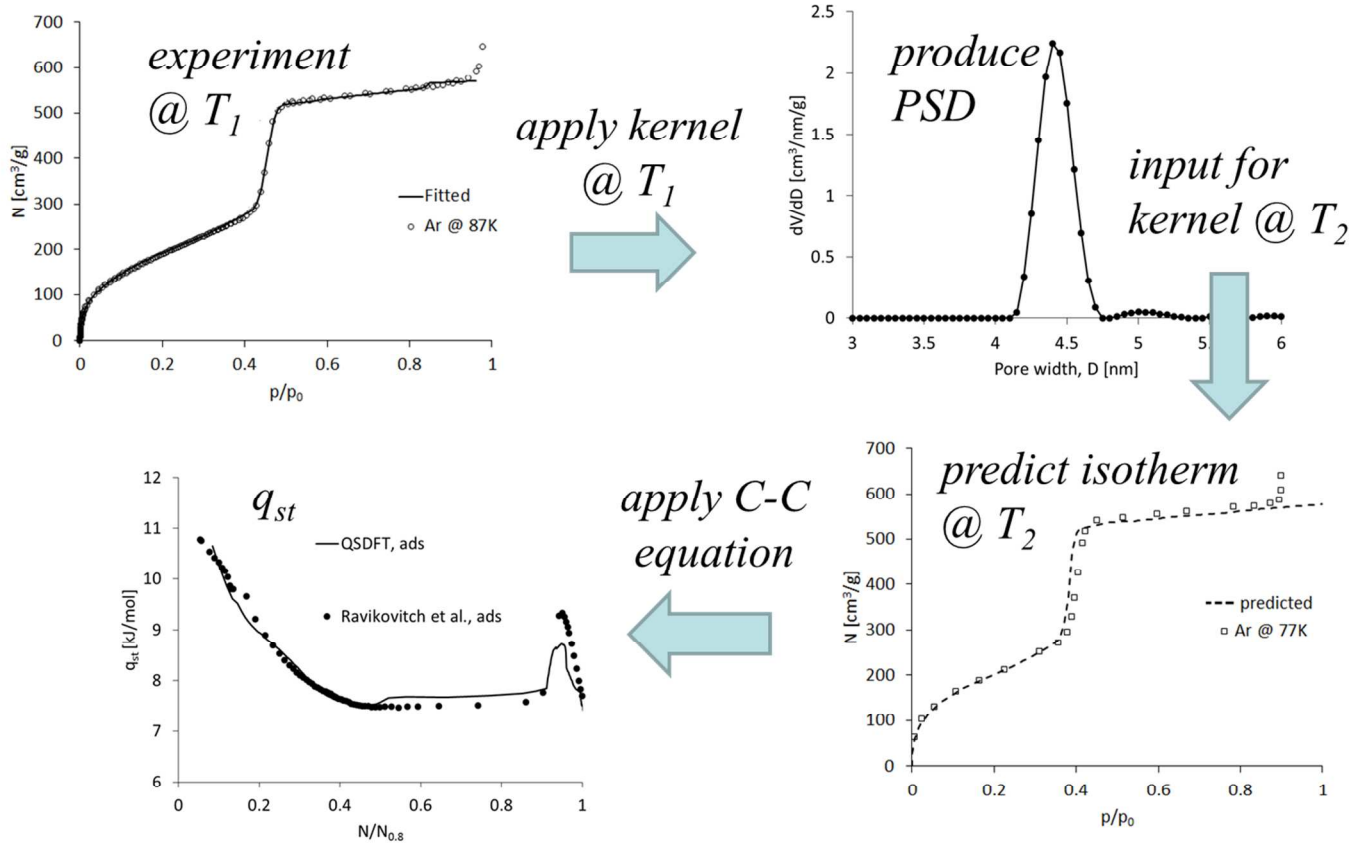

Fig. S2. Schematic of isosteric heat calculation procedure from the isotherm measured at one temperature, porous MCM-41 AM-5.

C. DFT and GCMC model parameters

Density Functional Theory

The accurate calculation of DFT isotherms relies on appropriate parameterization of the fluid-fluid $u_{ff}(|\mathbf{r}-\mathbf{r}'|)$ and fluid-solid $u_{sf}(|\mathbf{r}-\mathbf{r}'|)$ pair potentials, which must be tailored to the specific adsorbent-adsorbate combination. In both NLDFT and QSDFT methods, the fluid-fluid interactions are presented as Lennard-Jones potentials. Standard solid-fluid and fluid-fluid interaction parameters[1] were used in all the examples below for Ar and N_2 adsorption on carbon and silica.

DFT surface models

The NLDFT solid-fluid interaction potential takes the form of Steele's potential[2]. For the QSDFT isotherms, the solid-fluid interactions are presented as an integrated 9-3 Lennard-Jones potential[3] with the same σ_{sf} and ϵ_{sf} as for the NLDFT potential. As noted above, the QSDFT solid density ρ_s varies near the pore wall. The solid density is represented as a ramp function of the distance z from the pore wall:

$$\rho_s(z) = \begin{cases} \rho_s^0 & 0 \le z < h_0 \\ C\rho_s^0\left(1 - \dfrac{z-h_0}{2\delta}\right) & h_0 \le z < h_0 + 2\delta \\ 0 & h_0 + 2\delta < z \end{cases}$$

where h_0 = 2x0.34 nm is the thickness of the solid wall, C is a constant (C = 1 for silica and 0.75 for carbon[1])and δ is the roughness parameter[3, 4]. The interaction parameters for the adsorption examples in the Results and Discussion section are given below in Table S1.

	Adsorbent	Adsorbate	Fluid-Fluid Parameters		Solid-Fluid Parameters	
			ε_{ff}/k_B (K)	σ_{ff} (Å)	ε_{sf}/k_B (K)	σ_{sf} (Å)
NLDFT	carbon	N_2 at 77.4K	94.45	3.575	53.22	3.494
	carbon	Ar at 87.3K	118.05	3.305	55.0	3.35
QSDFT	carbon	N_2 at 77.4K	95.77	3.549	150	2.69
	silica	Ar at 87.3K	111.95	3.358	160.5	3.104

Table S1. Fluid-fluid and solid-fluid* interaction parameters for the examples in Section 4.

*Note – it is assumed in our modeling that the solid-fluid interactions for Ar and N_2 adsorption on carbon/silica do not vary significantly in the range of temperatures at which the isosteric heats are calculated. As such, the solid-fluid interactions are identical for the temperatures 76K-77.4K (N2) and 77.4-87.3K (Ar) used in the Results and Discussion section of the main text.

Grand Canonical Monte Carlo

For both N_2 and Ar, fluid-fluid interactions were truncated at 5.0 σ_{ff} without applying long-range corrections. Before GCMC simulations, the relation between pressure and chemical potential for each fluid was computed from canonical Monte Carlo simulations using the Widom particle insertion method[5]. At each point along the adsorption isotherm, the GCMC simulations were equilibrated using 3-4 $\times$ 10^7 Monte Carlo steps. The ensemble averages were computed from an additional 5-6 $\times$ 10^7 Monte Carlo steps. The final configuration from each adsorption point was used as a starting configuration for the next simulation.

GCMC Structural Models

Nonporous Carbon. As mentioned in the main text, the atomistic structural models of graphitized and disordered carbon surfaces were derived using the HRMC method[6, 7] based upon

radial density distribution determined from Madagascar graphite[6]. During GCMC simulation, carbon atoms were kept rigid and the interactions with either nitrogen molecules or argon atoms were computed using a single-site (12, 6) Lennard-Jones potential (see solid-fluid parameters shown in *supplementary information, section B*). The simulation box for nitrogen and argon adsorption on the model graphitized surface consisted of two identical carbon walls consisting of 13 graphene sheets separated by a distance of 6.0 nm[6]. The box was periodic in the in the *x* and *y* directions and the minimum image convention was applied to compute fluid-fluid interactions. The GCMC simulations of nitrogen adsorption on the morphologically disordered surface consisted of two identical carbon walls, each composed of 6 protruding graphene sheets generated from temperature-quench MC and separated by a minimal distance of 6.0 nm[6].

Mesoporous Silica. The solid-fluid potential for the structureless cylinder is given by an integrated potential[8]. The solid-fluid parameters were taken from the work of Vishnyakov and Neimark[9]. The simulation cell is represented by a periodic cylinder with the length 10.0 σ_{ff}. The internal pore diameters were matched to the mean-pore diameter as calculated by the DFT method. For the cylindrical pore model, we applied periodic boundary conditions and the minimum image convention in the longitudinal direction.

System	σ_{ff}(nm)	ε_{ff}/k_B [K]	σ_{sf}(nm)	ε_{sf}/k_B [K]
N_2-carbon (atomistic model)	0.3615	101.5	0.3494	53.22
Ar-carbon (atomistic model)	0.3405	119.8	0.3403	57.92
Ar-silica (structureless model)	0.3405	119.8	0.317	$\rho_s\varepsilon_{sf}/k_B$ [K/nm^2]
				2253.0

Table S2. Fluid-fluid and solid-fluid interaction parameters for GCMC simulations.

D. Hysteresis loops for MCM-41 samples

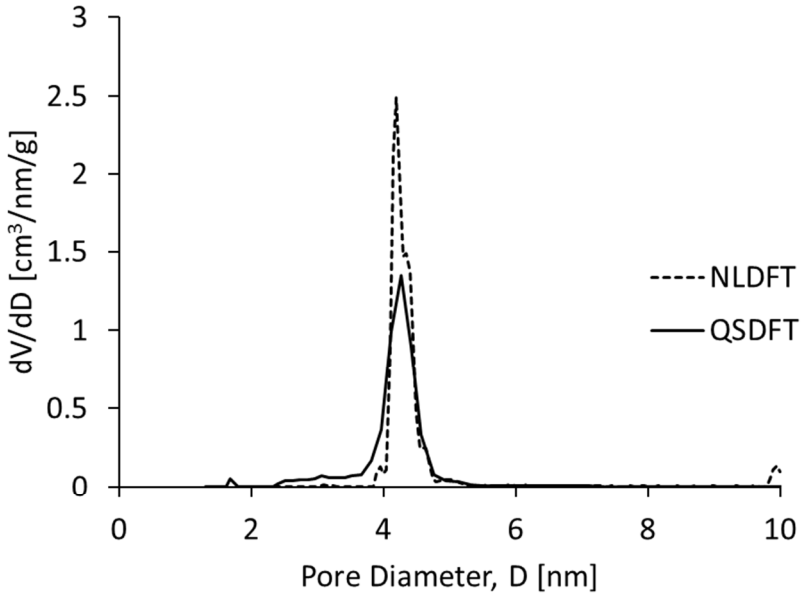

Fig. S3 Mesopore pore size distributions for the MCM-41 sample of Oliver.

Fig. S3 shows the mesopore pore size distribution for the MCM-41 sample measured by Oliver. The NLDFT and QSDFT distributions are in excellent agreement, with a mean pore size of 4.2nm.

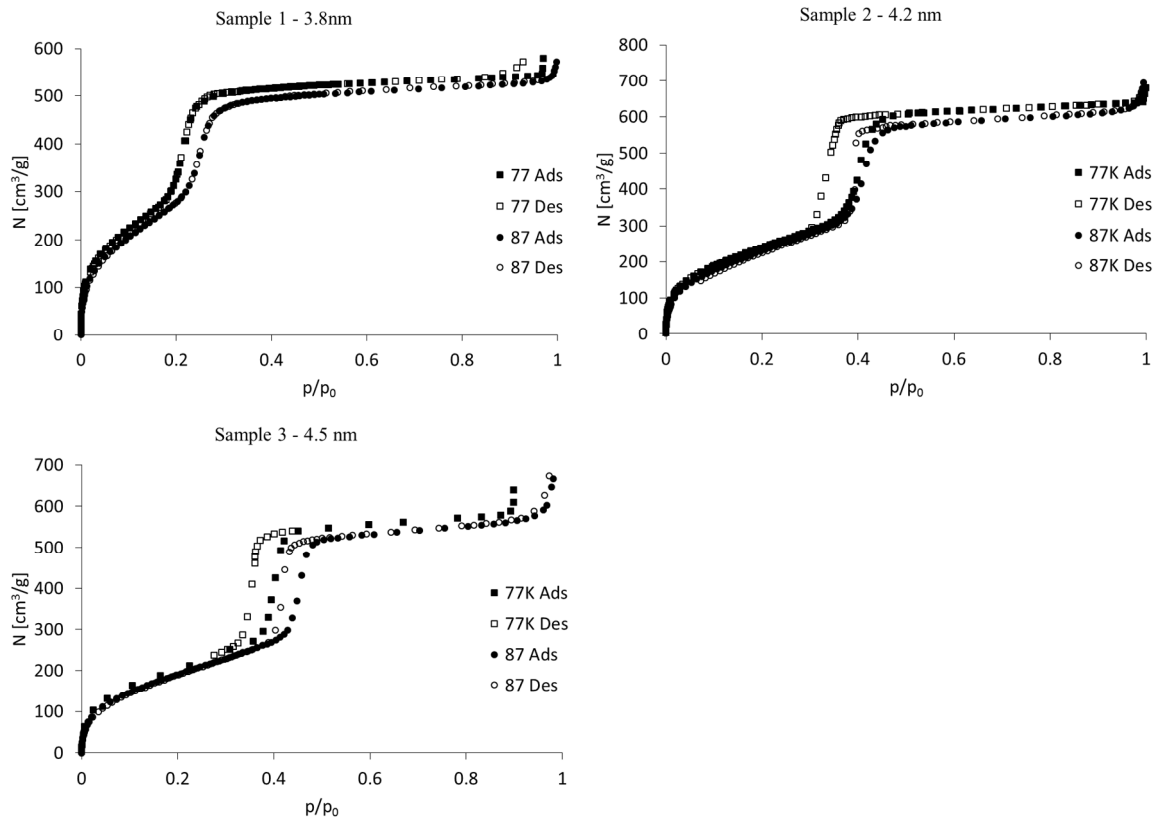

Fig. S4 Full hysteresis loops of all 3 MCM-41 samples in Fig. 5-6 in the main text.

Figure S4 shows the complete hysteresis loop for all three MCM-41 samples, illustrating the region of developing hysteresis @ 87K, as compared to fully developed hysteresis @ 77K. The smallest sample (AM-5 – 3.8nm) is completely reversible at both temperatures. MG-26 (4.2nm) has a large H1 type hysteresis at 77K, and a narrow hysteresis loop at 87K. The hysteresis loops are fully developed in C-50 (4.5nm).

SI References

1. Landers, J.; Gor, G. Y.; Neimark, A. V. Density functional theory methods for pore structure characterization: Review. *Colloids Surf., A* **2013,** *437*, 3-32.
2. Steele, W. A. The interaction of rare gas atoms with graphitized carbon black. *J. Phys. Chem.* **1978,** *82* (7), 817-821.
3. Neimark, A. V.; Lin, Y. Z.; Ravikovitch, P. I.; Thommes, M. Quenched solid density functional theory and pore size analysis of micro-mesoporous carbons. *Carbon* **2009,** *47* (7), 1617-1628.
4. Ravikovitch, P. I.; Neimark, A. V. Density functional theory model of adsorption on amorphous and microporous silica materials. *Langmuir* **2006,** *22* (26), 11171-11179.
5. Widom, B. Some topics in the theory of fluids. *J. Chem. Phys.* **1963,** *39* (11), 2808-2812.
6. Kowalczyk, P.; Gauden, P. A.; Furmaniak, S.; Terzyk, A. P.; Wiśniewski, M.; Ilnicka, A.; Łukaszewicz, J.; Burian, A.; Włoch, J.; Neimark, A. V. Morphologically disordered pore model for characterization of micro-mesoporous carbons. *Carbon* **2017,** *111*, 358-370.
7. Opletal, G.; Petersen, T. C.; Snook, I. K.; Russo, S. P. HRMC_2.0: Hybrid Reverse Monte Carlo method with silicon, carbon and germanium potentials. *Comput. Phys. Commun.* **2013,** *184* (8), 1946-1957.
8. Tanaka, H.; El-Merraoui, M.; Steele, W. A.; Kaneko, K. Methane adsorption on single-walled carbon nanotube: a density functional theory model. *Chem. Phys. Lett.* **2002,** *352*, 334.
9. Vishnyakov, A.; Neimark, A. V. Nucleation of liquid bridges and bubbles in nanoscale capillaries *J. Chem. Phys.* **2003,** *119*, 9755-9764.